# Identification and Functional Analysis of Serum Specific MiRNAs in Patients with Recurrent Aphthous Somatitis of Excess-heat or Yin-deficiency Syndrome

**Jie Bao**
Zhejiang Chinese Medical University
**Zhengyang Zhu**
Zhejiang Chinese Medical University
**Xizhao Zhang**
Zhejiang Chinese Medical University
**Lin Huang**
Zhejiang Chinese Medical University
**Li Xu**
Zhejiang Chinese Medical University
**Xiaobing Dou**
Zhejiang Chinese Medical University
**Yongsheng Fan** ( fyszjtcm@163.com )
Zhejiang Chinese Medical University

**Research article**

**Keywords:** recurrent aphthous stomatitis, microRNA, excess-heat syndrome, yin-deficiency syndrome

**Posted Date:** November 22nd, 2019

**DOI:** https://doi.org/10.21203/rs.2.17623/v1

# Abstract

Background. MiRNAs has become an important regulator in many processes. The purpose of our study is to screen the key serum miRNAs of different syndrome of recurrent aphthous stomatitis (RAS), to find new biomarkers for the diagnosis of RAS and to further explore their role in the pathogenesis of RAS.

Method. Serum samples were collected from patients meeting the RAS diagnostic criteria of excess-heat or yin-deficiency syndrome and healthy individuals. Core miRNAs were then identified under miRNA microarray analyses. Target prediction and bioinformatic analyses were carried out and gene-pathway-networks were visualized to better understand the relationship between different genes and pathways.

Result. (1) 90 individuals meeting the inclusion criteria were collected in this study, of which 30 were normal control, 30 were patients of excess-heat syndrome and the rest were patients of yin-deficiency syndrome. Among them, 9 miRNAs were screened out in excess-heat syndrome group, with 1 upregulated and 8 downregulated. And four random miRNAs (hsa-miR-20b-5p, hsa-miR-122-5p, hsa-miR-483-5p and hsa-miR-3197) were validated by real-time PCR method. 14 miRNAs were screened out in yin-deficiency syndrome group (7 upregulated and 7 downregulated). And hsa-miR-17-5p, hsa-miR-106-5p and hsa-miR-20b-5p were validated. (2) A total of 4776 target genes were identified for the validated 9 miRNAs in excess-heat syndrome group. These targets were enriched in GO categories including nervous system development, homophilic cell adhesion via plasma membrane adhesion molecules, and calcium ion binding and KEGG pathway such as proteoglycans in cancer, P13K-AKT signaling pathway and Calcium signaling pathway. 10172 target genes were identified for the validated 14 miRNAs in yin-deficiency syndrome group. The enriched GO categories included protein binding, positive regulation of transcription from RNA polymerase II promoter and membrane and enriched KEGG pathway included pathways in cancer, MAPK signaling pathway and Ras signaling pathway .

Conclusion. Hsa-miR-20b-5p in patients with RAS could act as the novel biomarker for clinical diagnosis of the disease. It is upregulated in RAS patients of excess-heat syndrome while downregulated in patients of yin-deficiency syndrome. The PI3K-Akt signaling pathway and MAPK signaling pathway and related target genes may provide new insights into the molecular mechanisms of excess-heat syndrome and yin-deficiency syndrome RAS, respectively.


# 1. Introduction

Recurrent aphthous stomatitis, also known as aphthous ulcer or ulcer, is the most common oral mucosal disease in all geographical regions (1). The prevalence of RAS in the general population is between 5 and 25% (2). So far, the pathogenesis of RAS is not clear, while it is considered to be multifactorial. Current studies have shown that genetic-mediated congenital and acquired immune disorders play an important role in the development of the disease (3). Traditional Chinese medicine (TCM) brings RAS into the category of “aphthous ulcer”, which can be divided into excess-heat syndrome and yin-deficiency syndrome according to different clinical manifestations. The excess-heat syndrome is generally

manifested as obvious pain, redness and swelling and other acute inflammation, which are accompanied by red tongue, yellow coating, and fast and powerful pulse; patients with yin-deficiency syndrome suffer a long disease course and chronic symptoms.

MicroRNAs (miRNAs) is a kind of evolutionarily conserved non-coding small molecule RNA, which mainly regulates the expression of protein coding genes through incomplete base pairing and has the function of regulating gene expression at the translation level (4). It has been estimated that more than 30% of human protein-coding genes are regulated by miRNAs (5). MiRNAs have emerged as vital regulators in many physiological and pathological processes in western medicine. There are few publications discussing the association of miRNA with the symptoms and diseases of TCM.

In this study, miRNA microarrays were used to investigate the miRNA expression profiles in the peripheral blood of RAS patients with excess-heat syndrome and yin-deficiency syndrome. Then, target genes were predicted and bioinformatic analysis was applied to interpret the core function. This paper aims to screen the key serum miRNAs present in excess-heat syndrome and yin-deficiency syndrome of RAS, which will identify novel biomarkers for clinical diagnosis of RAS and, further, their roles in the pathogenesis of this disease.

# 2. Materials And Methods

*2.1. Clinical sample collection.* Patients aged between 18 to 60 years old who meet the diagnostic criteria were enrolled in this study. Serum samples were collected from those patients and corresponding healthy subjects at the First Affiliated Hospital of Zhejiang Chinese Medical University from 2014–2016. Exclusion criteria consisted of underlying diseases, such as hypertension, diabetes and heart disease, drug therapy and other interventions. Blood was drawn at the outpatient clinic in the morning after fasting. This study was approved by Institutional Review Board of Zhejiang Chinese Medical University, and all the enrolled individuals signed informed consent. The blood was processed for serum extraction within 2 hours and then frozen into ultralow temperature freezer for long-term storage at –80°C. Clinical data were retrospectively collected from the medical records.

*2.2. Total RNA extraction and quality control.* Total RNA, including the miRNAs, was isolated from 500 µl serum using the Plasma/Serum Exosome Kit (Norgen, 42800), following the manufacturer's protocol. The RNA concentration was measured by Nanodrop 2000 spectrophotometer (Thermo Scientific) and stored at –80°C. RNA quality control was performed by realtime PCR with the following quality indicators: hsa-miR–16 and hsa-miR–192 (hsa-miR–16: 16–22hsa-miR–192: 25–30).

*2.3. MicroRNA microarrays.* We followed the methods of Chen et al. 2019 (6)and Fang et al. 2013 (7). MiRNA microarray analyses were performed on three groups: normal control group (NC Group), excess-heat syndrome of RAS (EH Group) and yin-deficiency syndrome of RAS (YD Group) according to the MiRNA Expression Profiling Assay Guide (LC Sciences, Hangzhou, China) (8, 9). Then, using poly (A) polymerase to make 4 to 8 µg total RNA sample poly (A) tail 3'-extended. An oligonucleotide tag was ligated to the poly (A) tail for later staining. Hybridization was performed overnight on a µParaflo

microfluidic chip with a microcirculation pump. On a microfluidic chip, each detection probe consists of a chemically modified nucleotide coding fragment, a complementary miRNA target or other target RNA and a polyethylene glycol spacer fragment to keep the coding fragment away from the substrate. The detection probe was synthesized in situ by PGR. The melting temperature of hybridization was balanced by detecting the chemical modification of the probe. 100L 6XSSPE buffer containing 25% formamide (0.90 M NaCl,60 mM $Na_2HPO_4$, 6 mM EDTA, pH 6.8) was hybridized at 34 ℃. After RNA hybridization, tag-conjugating Cy3 dye was circulated through the microfluidic chip for dye staining. Fluorescent images were collected using a laser scanner and the images were digitized using Array-Pro image analysis software. First subtract the background, and then use the LOWESS filter to normalize the signal to analyze the data (Locally-weighted Regression) (10).

*2.4. qRT-PCR for selected miRNAs.* Real-time PCR was performed on the individual samples in order to validate the miRNA profiling results of selected miRNAs using the two-step Stemaim-it miR qRT-PCR Quantitation Kit (SYBR Green) (Novland, Shanghai, China)with the BIO-RAD IQ5 real-time PCR instrument. Specific primers for mature miRNAs were obtained from Genepharm, Shanghai, China. All reactions were conducted in triplicate. Quantitative normalization was performed on U6 as an internal control. The fold-change of expression was calculated by using Ct values in comparison to controls. The expression levels were determined by the comparative ΔCt method.

*2.5. Target prediction and bioinformatic analyses.* Prediction of miRNA target genes in this study were carried out by using TargetScan and miRanda. The matches identified via the two programs were selected as the final target genes. Gene Ontology (GO) analysis was then applied to annotate the target genes of specified miRNAs, which participated in significant biological processes, molecular functions and cellular components (11). Two-sided Fisher's exact test was applied to classify the GO category, and the threshold of significance was defined by the *P*-value ($P < 0.05$). Similarly, Kyoto Encyclopedia of Genes and Genomes (KEGG) analysis was used to determine the significant pathway of the differential genes according to KEGG, and the same statistical method was used to select the significant pathways.

*2.6. Gene-pathway-Network.* To build a gene-pathway-network, the relationship between genes and pathways was calculated by their differential expression values; then, the results were visualized by CytoScape 3.6.1 software.

*2.7. qRT-PCR for specific genes.* Real-time PCR was performed to validate the specific genes according to the gene-pathway-network. Corresponding primers were also obtained from Genepharm, Shanghai, China. All the steps were referred to the 2.4 content above.

*2.8. Statistical Analysis.* SPSS 22.0 for Windows software was used for data analysis in this study. All the data were presented as the mean ± standard deviation. Comparisons between two groups were performed by Student's t-test if the variance was homogeneous. When the variance was not homogeneous, a nonparametric test was performed between two groups. $P<0.05$ was considered statistically significant.

# 3. Results

*3.1. General information of patients.* 90 patients met the inclusion criteria were collected in this study, of which 30 were normal control, 30 were excess-heat syndrome of RAS patients and the others were yin-deficiency syndrome. The ages were between 18 and 60 years old. 6 cases in each group were selected for microRNA microarrays, and the rest were applied for qRT-PCR validation. In the NC group, 16 cases were males and 14 were females. In the EH group, 13 were males and 17 were females while 15 were males and 15 were females in the YD group. There was no significant difference in the age between the three groups of patients (*P□0.05*). The average age of normal control group was (29.67±10.12) years old, the EH group was (31.57±10.59) and the YD group was (33.43±9.57). There was also no significant difference in the ages between the three groups (*P□0.05*) (Table 1).

*3.2. Differentially expressed miRNAs in excess-heat syndrome or yin-deficiency syndrome of RAS patients.*

The miRNA expression profiles of three groups were compared using MicroRNA Expression Profiling Assay (LC Sciences). Differentially expressed miRNAs were defined as those with *P*-values<0.05, and 131 miRNAs were differentially expressed in excess-heat syndrome of RAS patients compared to normal control patients; specifically, 78 miRNAs were upregulated, and 53 were downregulated (*P* <0.05). 37 miRNAs were differentially expressed in yin-deficiency syndrome of RAS patients as compared to normal control patients; specifically, 14 miRNAs were upregulation and, 23 were downregulation (*P* <0.05). To identify the significantly differentially expressed miRNAs, we established a signal value of >500 and a *P*-value of < 0.05 as the threshold for screening. Hsa-miR-20b-5p was screened out in both excess-heat syndrome and yin-deficiency syndrome of RAS patients (Fig 1). Interestingly, hsa-miR-20b-5p was upregulated in excess-heat syndrome of RAS patients, while it was downregulated in yin-deficiency syndrome of RAS patients. In total, 9 miRNAs were screened out in excess-heat syndrome, with 1 upregulated and 8 downregulated miRNAs. The results of hierarchical clustering of the 9 miRNAs were presented in the heat map diagram (Fig 1A). And 14 miRNAs were screened out in yin-deficiency syndrome, with 7 upregulated and 7 downregulated miRNAs. The results of hierarchical clustering of the 14 miRNAs were presented in the heat map diagram (Fig 1B).

3.3 *Validation of differentially expressed miRNAs by real-time PCR method*

To further confirm the results of the gene chips, the real-time fluorescence PCR method was used to verify the results. Three miRNAs (hsa-miR-122-5p, hsa-miR-483-5p and hsa-miR-3197) were randomly selected from the EH group, which were all significantly downregulated□fold change of >1.5□(Fig 2A).Two miRNAs (hsa-miR-17-5p and hsa-miR-106-5p) were randomly selected from the YD group, which demonstrated particularly significant downregulation□fold change of >1□(Fig 2B). Hsa-miR-20b-5p was upregulated in the EH group, and was particularly significantly downregulated in the YD group □fold change of >2□ (Fig

2C). The results showed a significant intragroup difference in the expression of miRNAs in a manner consistent with the data obtained from the microarray analysis.

*3.4. Bioinformatics analysis in excess-heat syndrome of RAS patients.*

A total of 4776 target genes were identified for the validated 9 miRNAs in the EH group. To better understand the potential implications of the differentially expressed miRNAs, GO analysis was carried out to evaluate their potential functions. GO categories included biological processes, cellular components and molecular functions. Nervous system development, homophilic cell adhesion via plasma membrane adhesion molecules, and calcium ion binding were the most significantly enriched for each of the categories (Fig 3A). To identify the biological pathways controlled by the involved miRNAs, we performed KEGG pathway enrichment analysis for the target genes and found that pathways in cancer were among the most enriched pathways. The PI3K-Akt signaling pathway, MAPK signaling pathway, and calcium signaling pathway also exhibited a significant difference (Fig 3B). A gene-pathway-network map was then constructed to describe the network of the most enriched pathways and related genes(Fig 3C). The PI3K-Akt signaling pathway played a key role in the network, connecting the target genes in directly or indirectly ways, especially PDGFRA, PRKCA, FGF2 and F2R.

*3.5. Bioinformatics analysis in yin-deficiency syndrome RAS patients.*

A total of 10172 target genes were identified for the validated 14 miRNAs in the YD group. Protein binding, positive regulation of transcription from RNA polymerase II promoter, and membrane were the most significantly enriched for each of the categories (Fig 4A). KEGG pathway enrichment analysis was then performed for the target genes and found that pathways in cancer was the most enriched pathway. The MAPK signaling pathway, PI3K-Akt signaling pathway, and Ras signaling pathway also exhibited significant differences (Fig 4B). A gene-pathway-network map was constructed to describe the network of the most enriched pathways and related genes (Fig 4C). The MAPK signaling pathway played a key role in the network, connecting the target genes, especially MAP2K1, ATK3, MAPK1, and FGF5.

*3.5. Validation of relevant expressed genes by real-time PCR method*

To confirm the results of the gene-pathway-network and further analysis, real-time PCR method was used. According to the literature and network map, corresponding genes were selected from EH group and YD group for in-depth analysis. PDGFRA selected from EH group was significantly upregulated（$P < 0.05$）, while MAP2K1 selected from the YD group was also upregulated without a significant difference relative to the NC group (Fig 5). The results suggest that there may be different core mechanisms between excess-heat syndrome and yin-deficiency syndrome of RAS patients.

# 4. Discussion

Recurrent aphthous stomatitis is a common oral mucosal disease characterized by pain, multiple, recurrent, small, oval or round necrotizing ulcers. It is the most common oral ulcerative disease, which usually occurs between the ages of 10 and 30 and recurs at different intervals (12). However, there is limited research regarding the pathogenesis of this disease. Since the regulation of miRNAs has been shown to correlate with various characteristics and prognosis in diseases, such as cancer and metastasis (4), acute respiratory distress syndrome (13), and hypoxic damage (14), this regulation may be helpful in uncovering the underlying mechanism in RAS pathogenesis. An ideal biomarker should be noninvasive, highly sensitive, highly specific, accurate, reliable, inexpensive, and reproducible. MiRNAs are promising potential biomarkers for disease because of their unique structure, high stability and specific expression patterns.

MiRNAs are small, single-stranded forms of RNA with a length of about 22 nucleotides. They are produced by the genome-encoded endogenously expressed hairpin-like precursor RNA. MiRNAs regulate protein code gene expression by interfering with either mRNA translation or targeting mRNA degradation (4). Since the first miRNA lin–4 was found by Victor Ambros and Gary Ruvkun in 1993 (15), the list of identified miRNAs has been growing rapidly. As of May 2019, 1917 human miRNA have been included in the miRbase. MiRNAs are capable of regulating diverse cellular processes, such as cell cycle progression, apoptosis, differentiation (16), and stress response, and play roles in organ development, metabolic homeostasis, tumor formation and metastasis, viral infection, the immune response, and so on.

In this study, 9 miRNAs (1 up-regulated and 8 down-regulated) were detected in the EH Group, compared with the NC Group. Among them, hsa-miR–20b–5p was significantly upregulated, and three miRNAs (hsa-miR–122–5p, hsa-miR–483–5p and hsa-miR–3197) were significantly downregulated. Additionally, 14 miRNAs (7 up-regulated and 7 down-regulated) were detected in the YD Group, and three miRNAs (hsa-miR–17–5p, hsa-miR–106–5p and hsa-miR–20b–5p) were significantly downregulated. Hsa-miR–20b–5p was obviously changed both in the EH Group and YD Group. Hsa-miR–20b–5p was upregulated in the EH Group and downregulated in the YD Group. The expression of the specified miRNAs identified in this study has been reported to be involved in different biological processes.

Lewkowicz et al. found that the production of IL–2, IFN- γ, TNF- α, IL–5, IL–6 and IL–8 in peripheral blood of RAS patients increased. On the contrary, the production of anti-inflammatory cytokines IL–10 and TGF-β decreased (17). Kemal Ozyurt et al. found that the levels of Th17 cytokines IL–17 and Th1 and Th2 cytokines were higher in RAS. IL–17 plays an important role in the immunity of all mucosa, especially oral mucosa (18). Hsa-miR–20b–5p, as a potential molecular biomarker of prognosis of CLL (chronic lymphoblastic leukemia), is also unbalanced in many B-cell lymphomas and T-cell leukemias. Hsa-miR–20a–5p and hsa-miR–20b–5p act as the hub of MS-related centers in multiple sclerosis, with each regulating approximately 500 genes. Many presumed target genes play a role in T cell activation and signal transduction, and have transcription factor activity (19). MiR–20b–5p can regulate important transcription factors, including hypoxia inducible factor 1 (HIF1) and signal transduction and activator of

transcription 3 (STAT3) (20). RAS and Behchet Syndrome (BD) have clinical and immunological characteristics in common (18). A Tulunay et al. suggested that JAK1/STAT3 signaling pathway may be activated by activating Th1/ Th17 cytokines such as IL–2, interferon (IFN- γ), IL–6, IL–17 and IL–23 (21). Ke Hu et al. have shown that STAT3 gene polymorphism is associated with susceptibility to BD in the Han population (22).

S Arikan et al. believe that lipid peroxidation and inadequate defense system seem to play a key role in the pathogenesis of recurrent aphthous stomatitis (23). Yunus Saral et al. found that the levels of vitamin A, E and C in serum and saliva of patients with RAS were significantly decreased, and the level of malondialdehyde (MDA) was significantly increased, which indicated that the non-enzymatic antioxidant capacity of patients with RAS was impaired (24). Z. Takci et al. showed that insulin resistance (IR) increased in patients with RAS, and IR was more prominent when the patients were in active stage (25). Extracellular miR–20b–5p derived from exosome is a circulating biomarker associated with type 2 diabetes mellitus, which regulates insulin-stimulated glucose metabolism through AKT signal transduction. Overexpression of miR–20b–5p decreased AKTIP abundance and insulin-stimulated glycogen accumulation (26). Jie Wu et al. found that activated T cells can play a key role in the defense response by up-regulating IL6 and STAT1, thus further affecting the progression of in breast cancer (BC). The BTN3A1-HAS-miR–20b–5p-HCP5 relationship may be the potential interaction mechanism between BC and immune cells (27). YIFAN LI et al. found that miR–20b–5p can inhibit renal cell carcinoma by regulating cell proliferation, migration and apoptosis (28). In conclusion, the participation of miR–20b–5p in T cell immune dysfunction, energy metabolism and inflammation may be the cause of RAS. MiR–20b–5p may be a new biomarker for clinical diagnosis of RAS in modern medicine and to distinguish between excess-heat syndrome and yin-deficiency syndrome of RAS.

Bioinformatics analysis showed that in excess-heat syndrome of RAS, the PI3K-Akt signaling pathway may play a key role in the gene-pathway-network map, connecting the target genes in direct or indirect ways, especially the PDGFRA gene. The PI3K-Akt signaling pathway and those target genes provide some hints when studying the mechanism of excess-heat syndrome of RAS. Zhang Bo et al. found that Shuizhongcao Granule can inhibit the expression of phosphorylated AKT and inhibit the activation of NF-κB, thus inhibiting inflammation. In addition, it can inhibit the ERK pathway, reduce the expression of IL–10 and IL–12b genes, and enhance the expression of IL–12a (29). Zichuan Zhang et al. found that the levels of superoxide dismutase (SOD), catalase (CAT) and glutathione peroxidase (GSHPx) in serum of patients with RAS were decreased, and the antioxidant defense system was impaired (30). Other studies have shown that nobiletin can reduce the levels of cTnI and MDA, increase the activity of serum SOD, reduce oxidative stress, and improve cardiac insufficiency induced by coronary artery microembolism by activating the PI3K/Akt pathway (31). Tangerine peel and Pinellia ternata may increase the level of SOD, decrease the level of MDA and SA-β-gal and reduce the formation of atherosclerotic plaque through PI3K/Akt pathway (32). Cheng Guo et al. have shown that AQP4 inhibitor TGN–020 has a detectable protective effect on lipopolysaccharide-induced lung injury, which is related to the inhibition of IL–17A through the downregulation of the PI3K/Akt signaling pathway and the upregulation of SOCS3 protein (33). The enhancement of energy metabolism leads to the decrease of AMPK activity and the activation

of the PI3K-AKT/mTOR signal pathway, which eventually leads to immune dysfunction and a series of RAS reactions.

In yin-deficiency syndrome of RAS, the MAPK signaling pathway played a key role in the network map connecting the target genes in directly or indirectly ways, especially the MAP2K1 gene. Li Ren et al. suggest that Kouyanqing granule can mediate the expression of p38MAPK protein, inhibit inflammatory reaction and regulate the level of growth factor to promote the healing of oral ulcer with yin deficiency (34). Slomiany BL et al. confirmed that Endothelin–1 (ET–1) can up-regulate leptin associated with oral ulcer healing through ETA receptor activation and MAPK/ERK signal transduction (35). Rafa S. Almeer et al. found that the fruit extract of Ziziphus jujuba could inhibit the oxidative stress and p38 MAPK expression of ulcerative colitis in rats by inducing the expression of Nrf2 and HO–1 (36). Liu Y et al. have shown that paeoniflorin can reduce reactive oxygen species and MDA produced by streptozotocin-treated INS–1 cells, increase the activity of SOD, and improve the injury of pancreatic β cells by inhibiting the p38MAPK and JNK signaling pathway (37). Wang L et al. have found that medicago sativa polysaccharides can reduce the oxidative stress induced by $H_2O_2$ in mouse embryonic fibroblasts by activating MAPK/Nrf2 signal transduction and inhibiting NF-κB signal transduction (38). In addition, the MAPK signaling pathway is an important inflammatory pathway. Atractylodin can inhibit inflammatory mediators through MAPK signaling pathway (39), and hydroxysafflor yellow A can inhibit the phosphorylation of JNK MAPK, p38 MAPK, and ERK MAPK (40). The participation of the MAPK pathway and its target genes in oxidative stress and immune regulation provides clues for the study of the pathogenesis of yin-deficiency.

# Conclusions

In conclusion, our results showed variations in serum miRNAs, especially regarding hsa-miR–20b–5p in patients with excess-heat syndrome and yin-deficiency syndrome of RAS. Furthermore, the PI3K-Akt signaling pathway and MAPK signaling pathway were revealed to be closely related with excess-heat syndrome and yin-deficiency syndrome, respectively. Hsa-miR–20b–5p may be a novel biomarker for clinical diagnosis of RAS, and its pathways and target genes can provide new insights into the molecular mechanisms underlying the disease and new targets for the prevention and treatment of RAS.

# Abbreviations

RAS: recurrent aphthous stomatitis; TCM: Traditional Chinese medicine; NC: normal control; EH: excess-heat; YD: yin-deficiency.

# Declarations

# Acknowledgements

Not applicable.

## Ethics approval and consent to participate

This study was approved by Institutional Review Board of Zhejiang Chinese Medical University. Informed consent obtained from all participants was written.

## Authors' contributions

J. Bao and Z. Y. Zhu contributed to conception and drafted the manuscript; X. Z. Zhang, L. Xu, X. B. Dou and L. Huang contributed to data conduct and analysis; Y. S. Fan and J. Bao contributed to design and critically revised the manuscript. All authors above gave final approval and agreed to be accountable for all aspects of the study.

## Data Availability Statement

The data used to support the findings of this study are involve patient privacy and have not yet been provided, they can be obtained from the appropriate author.

## Funding

This work was supported by National Basic Research Program of China (973 Program) (2014CB543000), the Youth Program of National Natural Science Foundation of China (Grant nos. 81803980) and the Youth Program of National Natural Science Foundation of Zhejiang Province(Grant nos. LQ18H270004).

## Consent for publication

Not Applicable.

## Competing Interests

The authors declare that they have no competing interests.

## References

1.Bilodeau EA, Lalla RV. Recurrent oral ulceration: Etiology, classification, management, and diagnostic algorithm. Periodontol 2000. 2019;80(1):49–60.

2.Slebioda Z, Szponar E, Kowalska A. Etiopathogenesis of recurrent aphthous stomatitis and the role of immunologic aspects: literature review. Arch Immunol Ther Exp (Warsz). 2014;62(3):205–15.

3.Dudding T, Haworth S, Lind PA, Sathirapongsasuti JF, andMe Research T, Tung JY, et al. Genome wide analysis for mouth ulcers identifies associations at immune regulatory loci. Nat Commun. 2019;10(1):1052.

4.Ma L. MicroRNA and Metastasis. Adv Cancer Res. 2016;132:165–207.

5.Bartel DP. MicroRNAs: genomics, biogenesis, mechanism, and function. Cell. 2004;116(2):281–97.

6.Chen Q, Wu X, Gao X, Song H, Zhu X. Development and Validation of an Ultra-Performance Liquid Chromatography Method for the Determination of Wedelolactone in Rat Plasma and its Application in a Pharmacokinetic Study. Molecules. 2019;24(4).

7.Fang X, Zhao Y, Ma Q, Huang Y, Wang P, Zhang J, et al. Identification and comparative analysis of cadmium tolerance-associated miRNAs and their targets in two soybean genotypes. PLoS One. 2013;8(12):e81471.

8.Gao X, Gulari E, Zhou X. In situ synthesis of oligonucleotide microarrays. Biopolymers. 2004;73(5):579–96.

9.Zhu Q, Hong A, Sheng N, Zhang X, Matejko A, Jun KY, et al. microParaflo biochip for nucleic acid and protein analysis. Methods in molecular biology (Clifton, NJ). 2007;382:287–312.

10.Bolstad BM, Irizarry RA, Astrand M, Speed TP. A comparison of normalization methods for high density oligonucleotide array data based on variance and bias. Bioinformatics (Oxford, England). 2003;19(2):185–93.

11.Gene Ontology C. The Gene Ontology project in 2008. Nucleic Acids Res. 2008;36(Database issue):D440–4.

12.Kayabasi S, Kuzucu I. A novel prognostic biomarker for recurrent aphthous stomatitis: calprotectin. J Laryngol Otol. 2019;133(8):691–5.

13.Ke XF, Fang J, Wu XN, Yu CH. MicroRNA–203 accelerates apoptosis in LPS-stimulated alveolar epithelial cells by targeting PIK3CA. Biochem Biophys Res Commun. 2014;450(4):1297–303.

14.Liu C, Zhao L, Han S, Li J, Li D. Identification and Functional Analysis of MicroRNAs in Mice following Focal Cerebral Ischemia Injury. Int J Mol Sci. 2015;16(10):24302–18.

15.Lee RC, Feinbaum RL, Ambros V. The C. elegans heterochronic gene lin–4 encodes small RNAs with antisense complementarity to lin–14. Cell. 1993;75(5):843–54.

16.Huang Y, Shen XJ, Zou Q, Wang SP, Tang SM, Zhang GZ. Biological functions of microRNAs: a review. J Physiol Biochem. 2011;67(1):129–39.

17.Lewkowicz N, Lewkowicz P, Banasik M, Kurnatowska A, Tchorzewski H. Predominance of Type 1 cytokines and decreased number of CD4(+)CD25(+high) T regulatory cells in peripheral blood of patients with recurrent aphthous ulcerations. Immunol Lett. 2005;99(1):57–62.

18.Ozyurt K, Celik A, Sayarlioglu M, Colgecen E, Inci R, Karakas T, et al. Serum Th1, Th2 and Th17 cytokine profiles and alpha-enolase levels in recurrent aphthous stomatitis. J Oral Pathol Med. 2014;43(9):691–5.

19.Angerstein C, Hecker M, Paap BK, Koczan D, Thamilarasan M, Thiesen HJ, et al. Integration of MicroRNA databases to study MicroRNAs associated with multiple sclerosis. Mol Neurobiol. 2012;45(3):520–35.

20.Papageorgiou SG, Kontos CK, Tsiakanikas P, Stavroulaki G, Bouchla A, Vasilatou D, et al. Elevated miR–20b–5p expression in peripheral blood mononuclear cells: A novel, independent molecular biomarker of favorable prognosis in chronic lymphocytic leukemia. Leuk Res. 2018;70:1–7.

21.Tulunay A, Dozmorov MG, Ture-Ozdemir F, Yilmaz V, Eksioglu-Demiralp E, Alibaz-Oner F, et al. Activation of the JAK/STAT pathway in Behcet's disease. Genes Immun. 2015;16(2):170–5.

22.Hu K, Hou S, Jiang Z, Kijlstra A, Yang P. JAK2 and STAT3 polymorphisms in a Han Chinese population with Behcet's disease. Invest Ophthalmol Vis Sci. 2012;53(1):538–41.

23.Arikan S, Durusoy C, Akalin N, Haberal A, Seckin D. Oxidant/antioxidant status in recurrent aphthous stomatitis. Oral Dis. 2009;15(7):512–5.

24.Saral Y, Coskun BK, Ozturk P, Karatas F, Ayar A. Assessment of salivary and serum antioxidant vitamins and lipid peroxidation in patients with recurrent aphthous ulceration. The Tohoku journal of experimental medicine. 2005;206(4):305–12.

25.Takci Z, Karadag AS, Ertugrul DT, Bilgili SG. Elevated insulin resistance in patients with recurrent aphthous stomatitis. Clin Oral Investig. 2015;19(6):1193–7.

26.Katayama M, Wiklander OPB, Fritz T, Caidahl K, El-Andaloussi S, Zierath JR, et al. Circulating Exosomal miR–20b–5p Is Elevated in Type 2 Diabetes and Could Impair Insulin Action in Human Skeletal Muscle. Diabetes. 2019;68(3):515–26.

27.Wu J, Li M, Zhang Y, Cai Y, Zhao G. Molecular mechanism of activated T cells in breast cancer. Onco Targets Ther. 2018;11:5015–24.

28.Li Y, Chen D, Jin L, Liu J, Su Z, Li Y, et al. MicroRNA–20b–5p functions as a tumor suppressor in renal cell carcinoma by regulating cellular proliferation, migration and apoptosis. Mol Med Rep. 2016;13(2):1895–901.

29.Bo Z, Xiang Q, Shan-Ming R, Wang B, De-Hou D, Liang X, et al. Investigation on Molecular Mechanism of Fibroblast Regulation and the Treatment of Recurrent Oral Ulcer by Shuizhongcao Granule-Containing Serum. Evid Based Complement Alternat Med. 2015;2015:324091.

30.Zhang Z, Li S, Fang H. Enzymatic antioxidants status in patients with recurrent aphthous stomatitis. J Oral Pathol Med. 2017;46(9):817–20.

31.Mao Q, Liang X, Wu Y, Lu Y. Nobiletin protects against myocardial injury and myocardial apoptosis following coronary microembolization via activating PI3K/Akt pathway in rats. Naunyn Schmiedebergs Arch Pharmacol. 2019.

32.Yu Y, Bai F, Liu Y, Yang Y, Yuan Q, Zou D, et al. Fibroblast growth factor (FGF21) protects mouse liver against D-galactose-induced oxidative stress and apoptosis via activating Nrf2 and PI3K/Akt pathways. Mol Cell Biochem. 2015;403(1–2):287–99.

33.Guo C, Wu T, Zhu H, Gao L. Aquaporin 4 Blockade Attenuates Acute Lung Injury Through Inhibition of Th17 Cell Proliferation in Mice. Inflammation. 2019;42(4):1401–12.

34.Li REN, Ren'an QIN, JiANDong LUO, Deqin WANG. REN Li QIN Ren'an LUO JiANDong WANG Deqin. Traditional Chinese Drug Research and Clinical Pharmacology 2018,29(04):387–392.

35.Slomiany BL, Slomiany A. Role of endothelin–1-dependent up-regulation of leptin in oral mucosal repair. Journal of physiology and pharmacology: an official journal of the Polish Physiological Society. 2005;56(4):531–41.

36.Almeer RS, Mahmoud SM, Amin HK, Abdel Moneim AE. Ziziphus spina-christi fruit extract suppresses oxidative stress and p38 MAPK expression in ulcerative colitis in rats via induction of Nrf2 and HO–1 expression. Food Chem Toxicol. 2018;115:49–62.

37.Liu Y, Han J, Zhou Z, Li D. Paeoniflorin protects pancreatic beta cells from STZ-induced damage through inhibition of the p38 MAPK and JNK signaling pathways. Eur J Pharmacol. 2019;853:18–24.

38.Wang L, Xie Y, Yang W, Yang Z, Jiang S, Zhang C, et al. Alfalfa polysaccharide prevents H2O2-induced oxidative damage in MEFs by activating MAPK/Nrf2 signaling pathways and suppressing NF-kappaB signaling pathways. Sci Rep. 2019;9(1):1782.

39.Lyu Z, Ji X, Chen G, An B. Atractylodin ameliorates lipopolysaccharide and d-galactosamine-induced acute liver failure via the suppression of inflammation and oxidative stress. Int Immunopharmacol. 2019;72:348–57.

40.Zheng M, Guo X, Pan R, Gao J, Zang B, Jin M. Hydroxysafflor Yellow A Alleviates Ovalbumin-Induced Asthma in a Guinea Pig Model by Attenuateing the Expression of Inflammatory Cytokines and Signal Transduction. Front Pharmacol. 2019;10:328.

# Table

Table 1. Basic information of the three sample groups

| | N | Gender | | Age |
|---|---|---|---|---|
| | | Male | Female | |
| NC Group | 30 | 16 | 14 | 29.67±10.12 |
| EH Group | 30 | 13 | 17 | 31.57±10.59 |
| YD Group | 30 | 15 | 15 | 33.43±9.57 |

# Figures

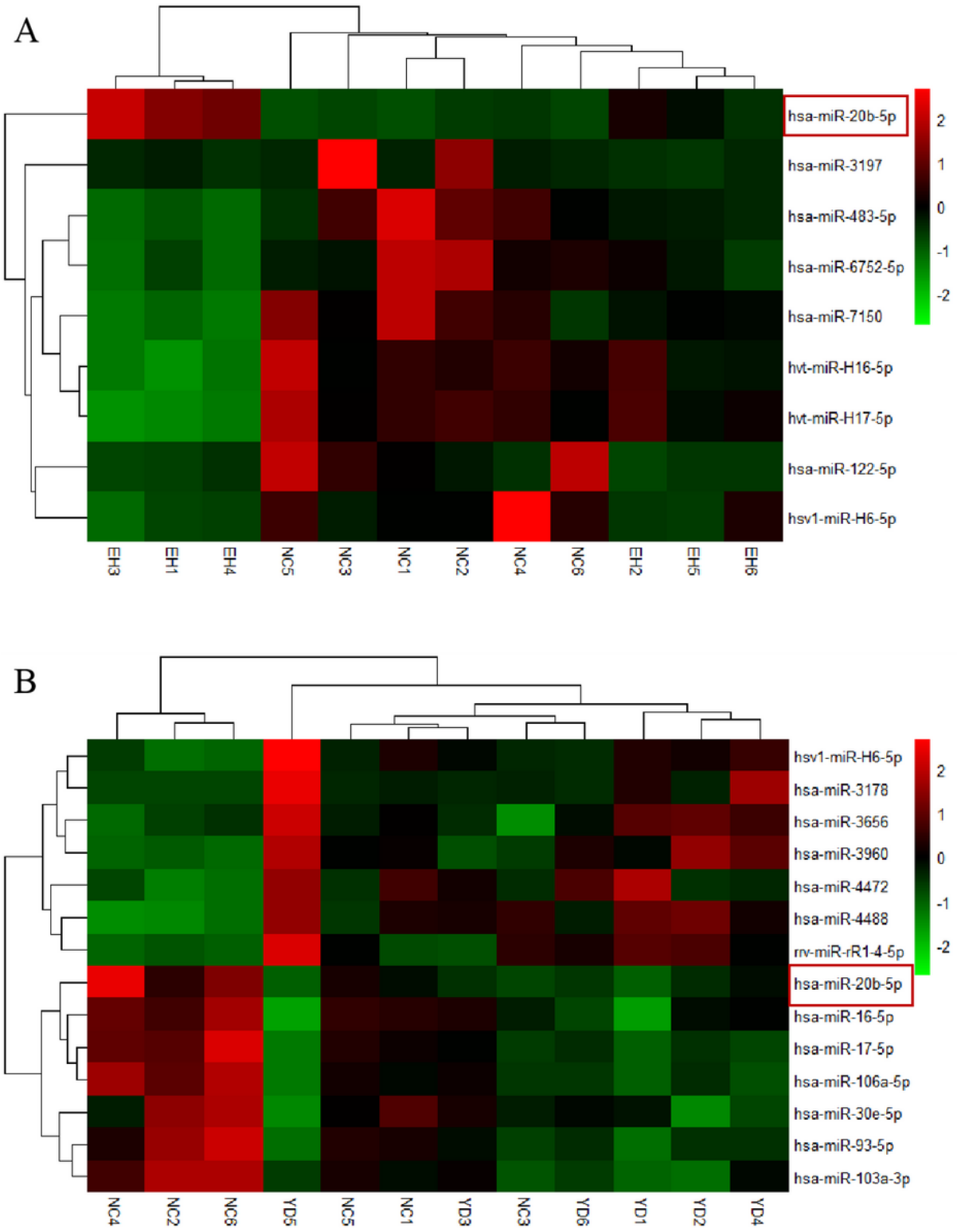


## Figure 1

Figure 1A. Heat map and hierarchical cluster analysis of the altered miRNAs in excess-heat syndrome RAS of patients, compared with normal control group. Figure 1B. Heat map and hierarchical cluster analysis of the altered miRNAs in yin-deficiency syndrome of RAS patients, compared with normal control group. The color code in each heat map is linear, with green as the lowest, and red as the highest. The average signals of the changed miRNAs in each of the two groups were clustered using a Euclidean

distance function. The miRNAs with the most similar expression patterns were placed next to each other (n = 6 per group).

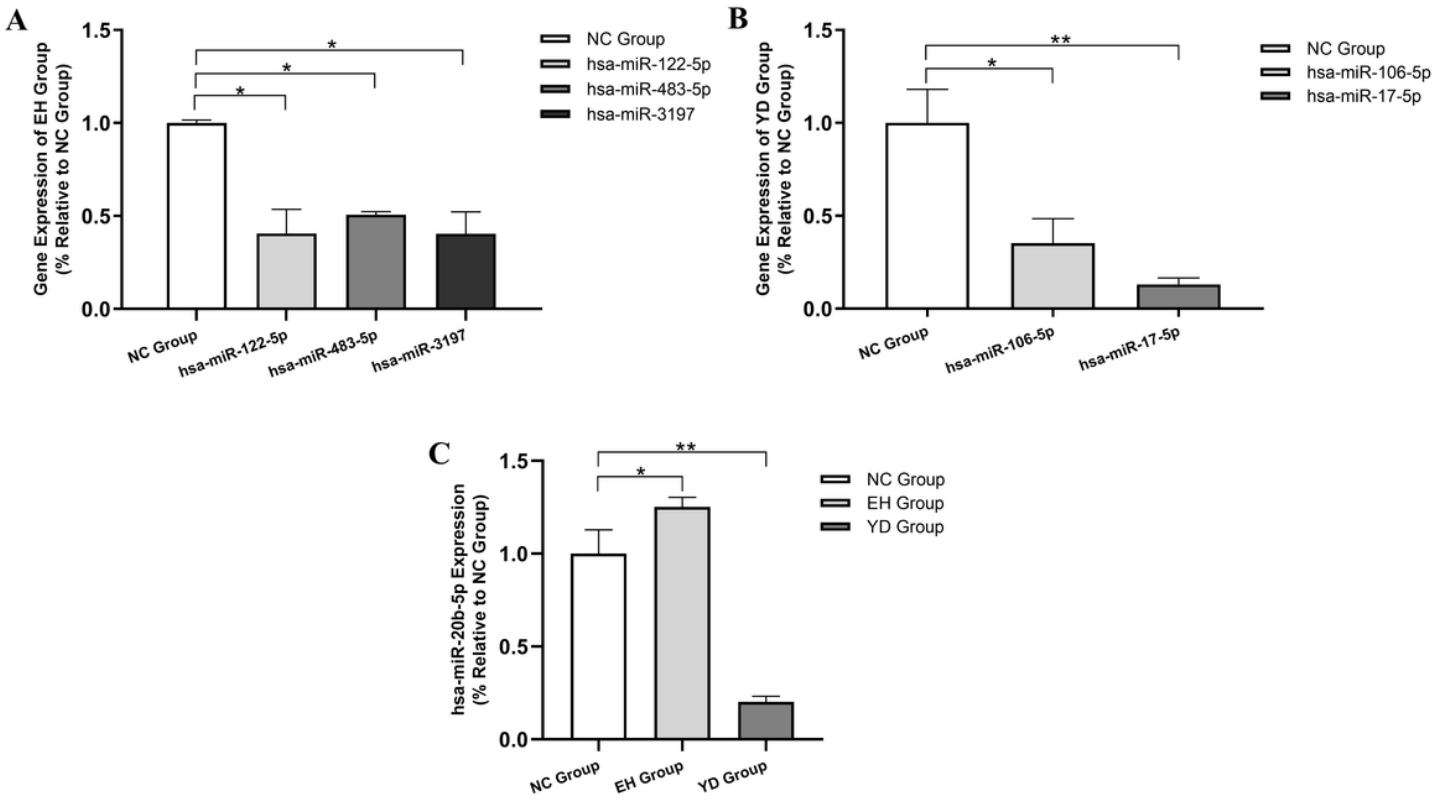


## Figure 2

Figure 2A. Gene expressions of three random miRNAs selected from the EH group were confirmed by real time RT-PCR method. Figure 2B. Gene expressions of two random miRNAs selected from the YD group were confirmed by real time RT-PCR method. Figure 2C. Hsa-miR-20b-5p of both EH group and YD group was confirmed by real time RT-PCR method respectively. Each corresponding control of the verified miRNA with change is normalized as 1. Each test was in triplicates and U6 was used as internal control. The bars represent the mean ± SE, and n = 30 per group. Compared with NC Group, *p < 0.05, **p < 0.01.

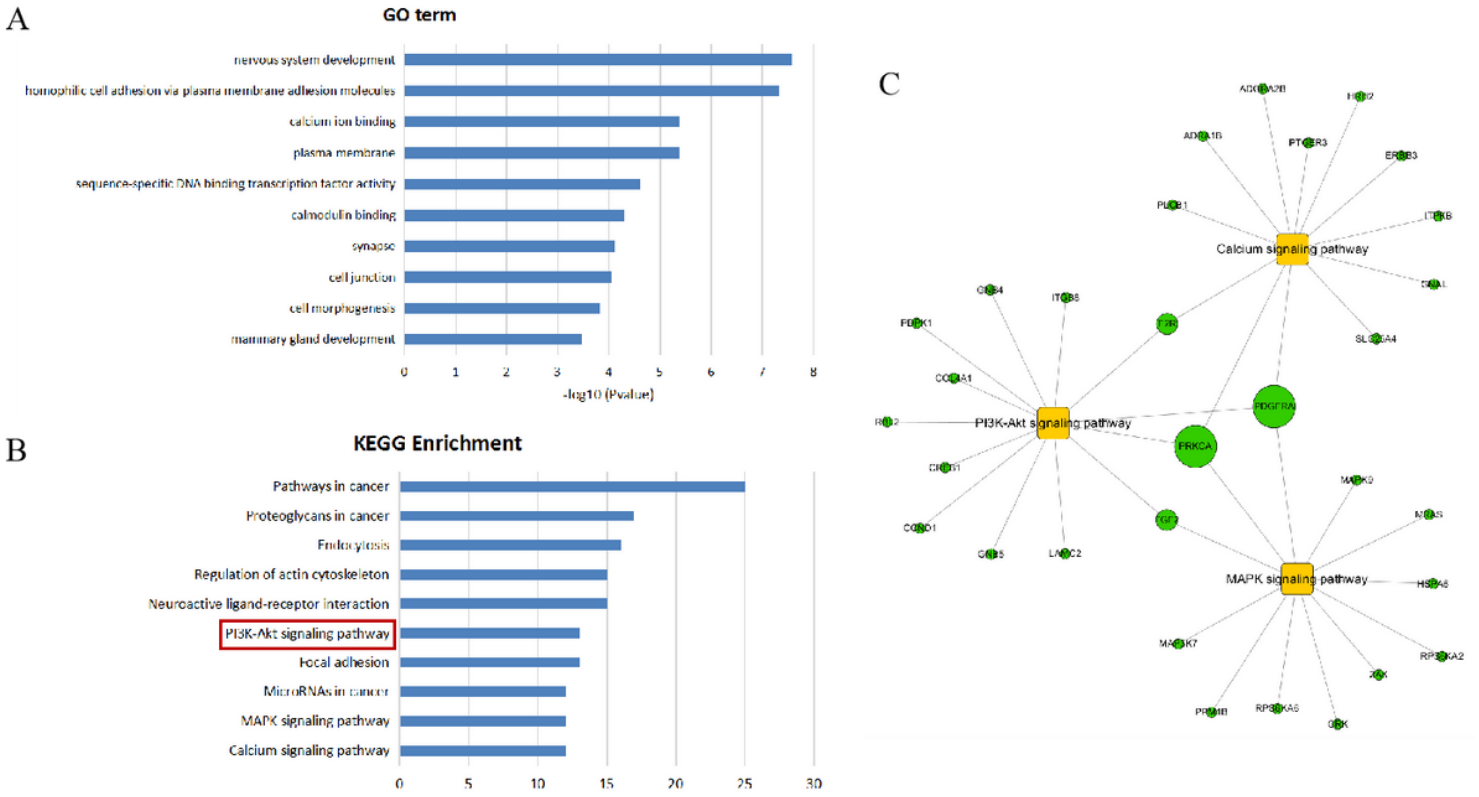


## Figure 3

Figure 3A. Target genes of the altered miRNAs annotated significant GOs in excess-heat syndrome of RAS patients, compared with normal control group. The vertical and horizontal axes are the GO terms and the –Log10 of GOs, respectively. Log is the logarithm of the P value and $P < 0.05$ is considered significant. Figure 3B. Target genes of the altered miRNAs annotated significant pathways in excess-heat syndrome of RAS patients, compared with normal control group. The vertical and horizontal axes are the pathway terms and the -Log10 of pathways, respectively. Log is the logarithm of P value and $P < 0.05$ is considered significant. Figure 3C. The gene-pathway-network of the specified pathways in excess-heat syndrome of RAS patients, compared with normal control group. The yellow squares indicate the significant pathways, and green circles indicate the genes. Furthermore, gray lines indicate the relationship between each other.

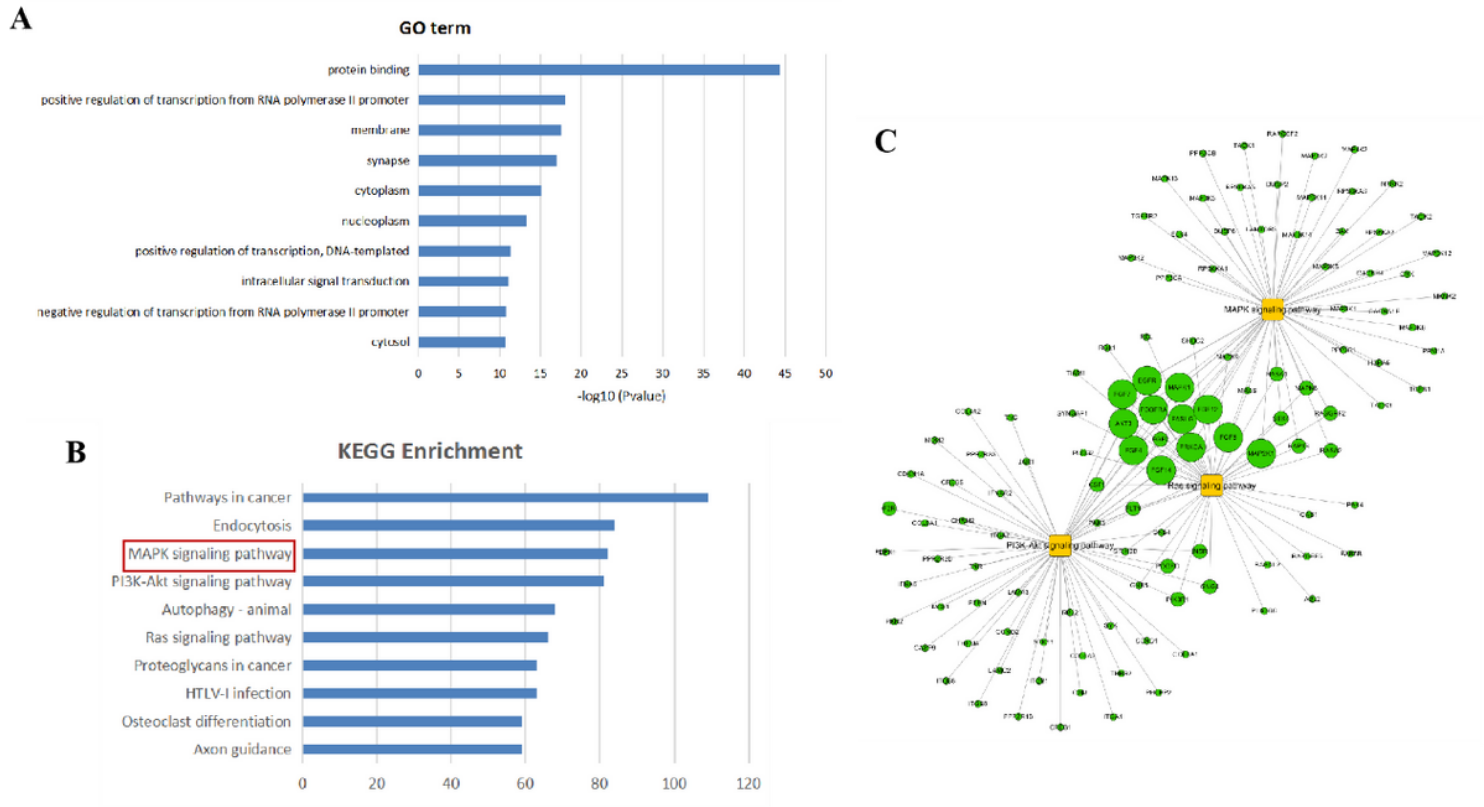


## Figure 4

Figure 4A. Target genes of the altered miRNAs annotated significant GOs in yin-deficiency syndrome of RAS patients, compared with normal control group. The vertical and horizontal axes are the GO terms and the –Log10 of GOs, respectively. Log is the logarithm of the P value and $P < 0.05$ is considered significant. Figure 4B. Target genes of the altered miRNAs annotated significant pathways in yin-deficiency syndrome of RAS patients, compared with normal control group. The vertical and horizontal axes are the pathway terms and the -Log10 of pathways, respectively. Log is the logarithm of P value and $P < 0.05$ is considered significant. Figure 4C. The gene-pathway-network of the specified pathways in yin-deficiency syndrome of RAS patients, compared with normal control group. The yellow squares indicate the significant pathways, and green circles indicate the genes. Furthermore, gray lines indicate the relationship between each other.

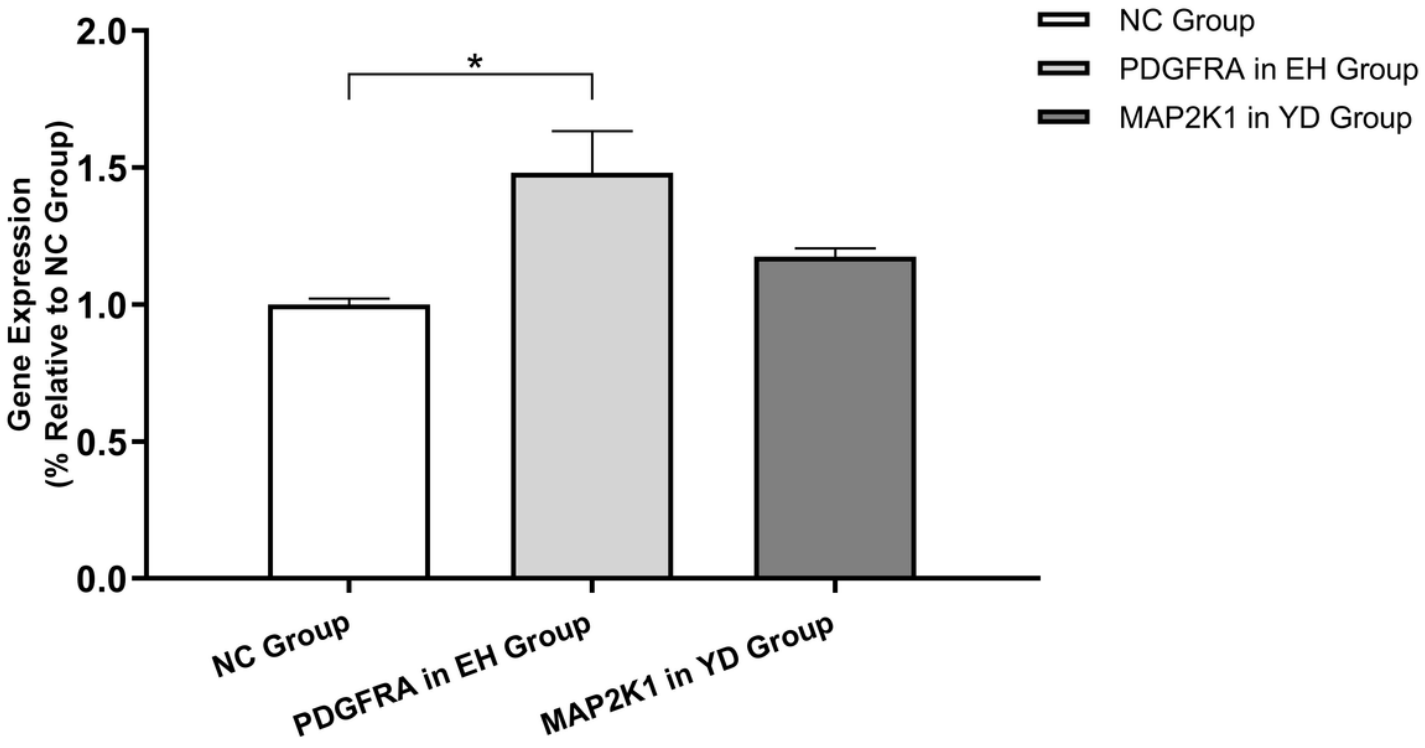


## Figure 5

The expression of related genes on the core pathways were detected by real time RT-PCR method. Each corresponding control of the verified gene with change is normalized as 1. Each test was in triplicates and GAPDH was used as internal control. The bars represent the mean ± SE, and n = 30 per group. Compared with NC Group, *P < 0.05.